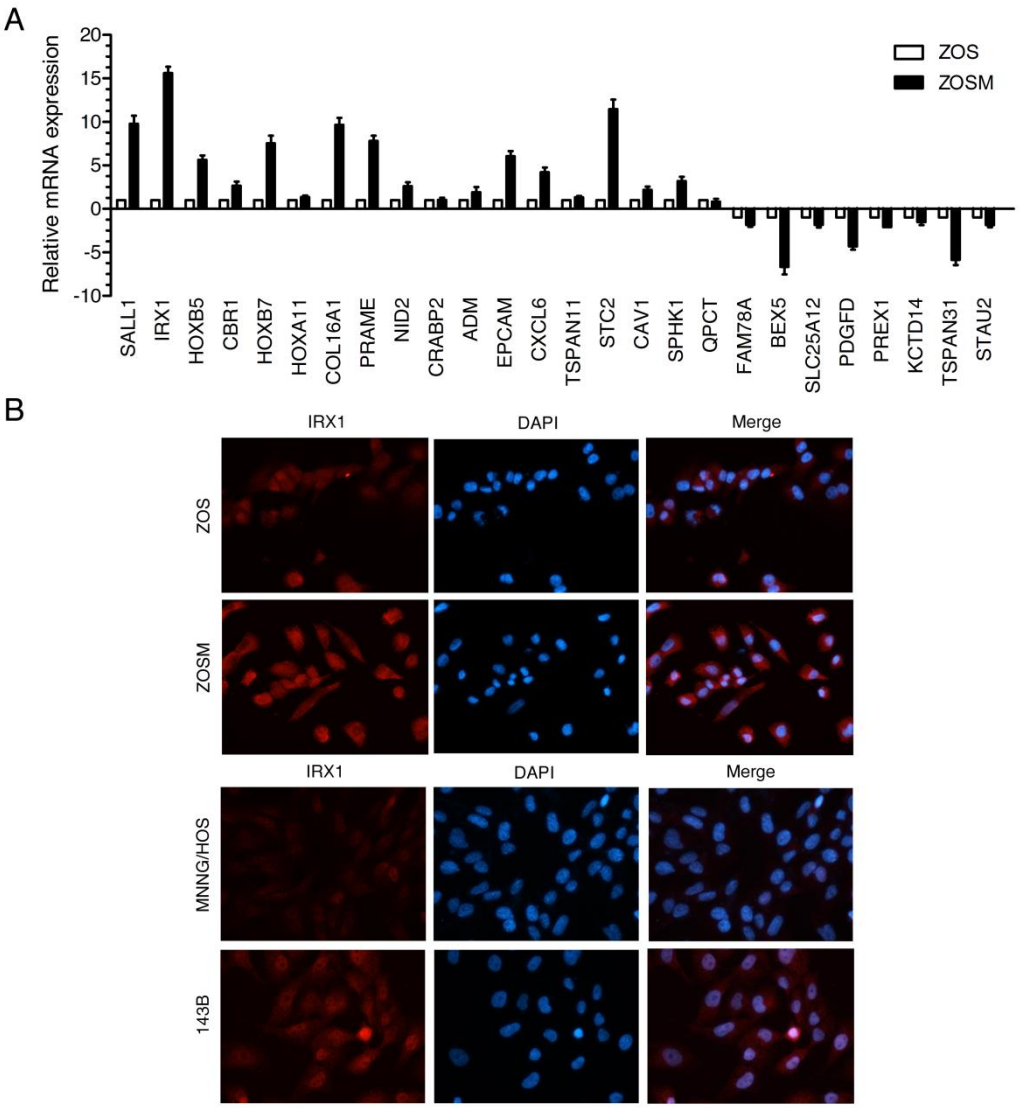

Supplemental Figure 1

Gene expression in ZOS and ZOSM cells. (A) The mRNA expression levels of the indicated genes were determined in ZOS and ZOSM cells using real-time PCR. The values shown are the mean ± SD of 3 separate determinations. (B) IRX1 protein expression in primary and commercially available osteosarcoma cell lines was detected by immunofluorescence (×400 magnification).

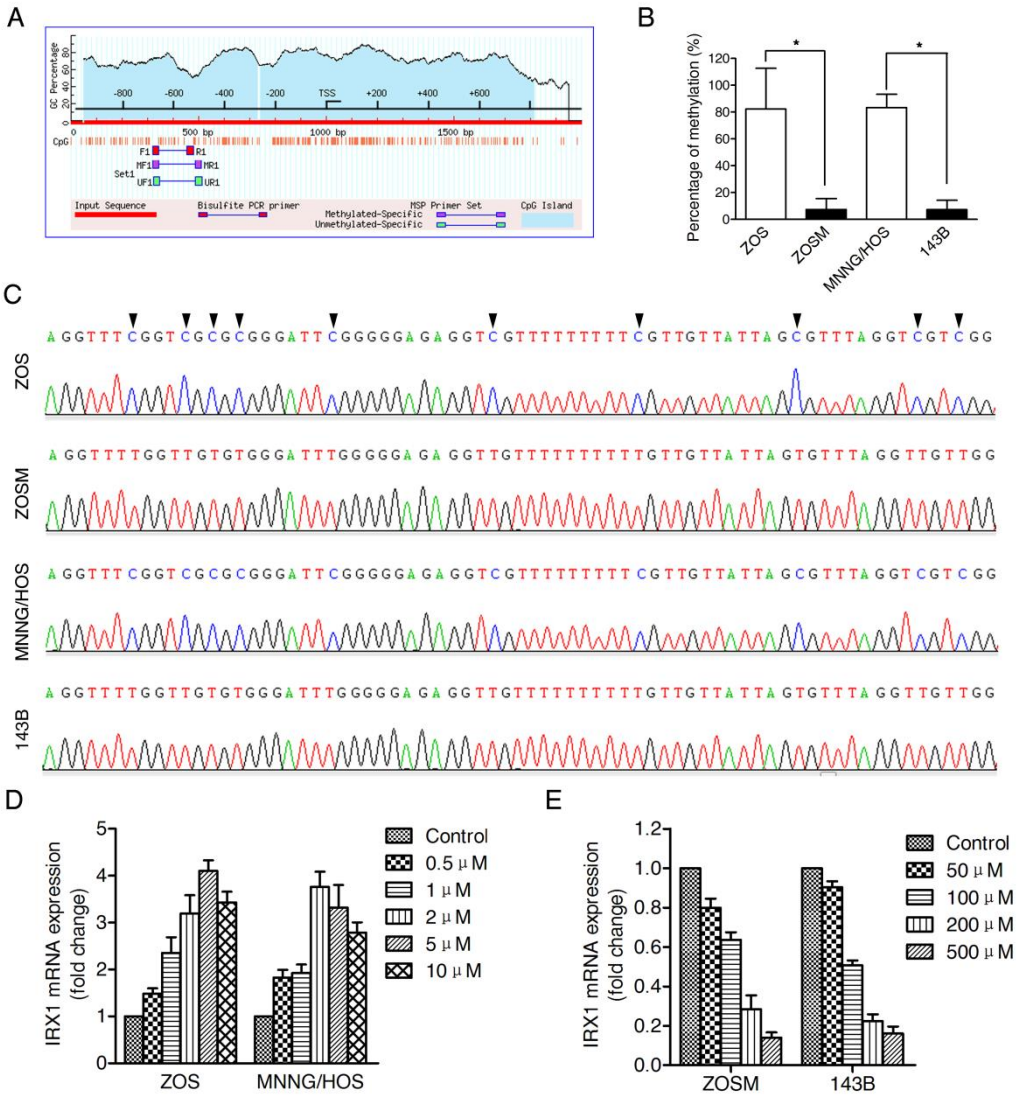

Supplemental Figure 2

IRX1 expression was associated with promoter hypomethylation. (A) Schematic map of CpG sites within the CpG islands in the IRX1 promoter by methylation analysis. (B) The methylation status of the IRX1 promoter region (-521 to -679) in ZOS and ZOSM cells was analyzed by bisulfite sequencing PCR. (C) Representative sequencing results of PCR products amplified from bisulfite converted DNA from osteosarcoma cells. The arrows indicate the CpG sites. (D) IRX1 mRNA expression was determined by real-time PCR after treatment with varying concentrations (0.5, 1, 2, 5, 10μM) of DAC. (E) IRX1 mRNA expression was determined by real-time PCR after treatment with varying concentrations (50, 100, 200, 500μM) of AdoMet for 6 days. Results shown in D and E are the mean ± SD (n=3). *P<0.05.

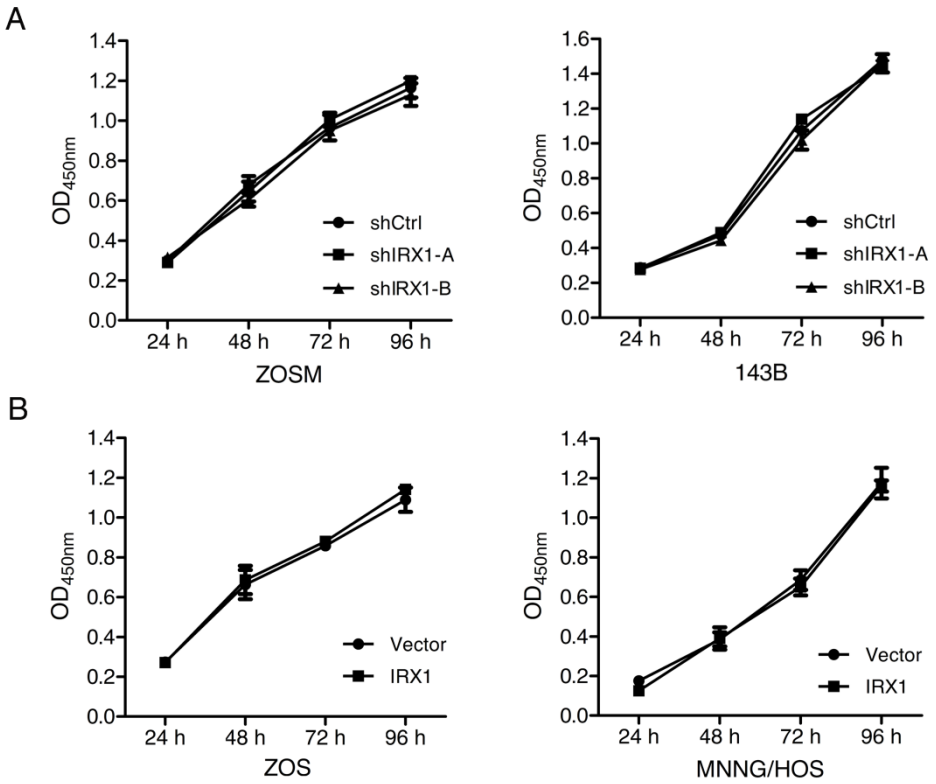

Supplemental Figure 3

IRX1 did not affect osteosarcoma cell growth. (A) A Cell Counting Kit-8 assay was performed on control and IRX1-knockdown ZOSM and 143B cells. (B) A Cell Counting Kit-8 assay was performed on control and IRX1-overexpressing ZOS and MNNG/HOS cells. The values shown are the mean ± SD of 3 separate determinations.

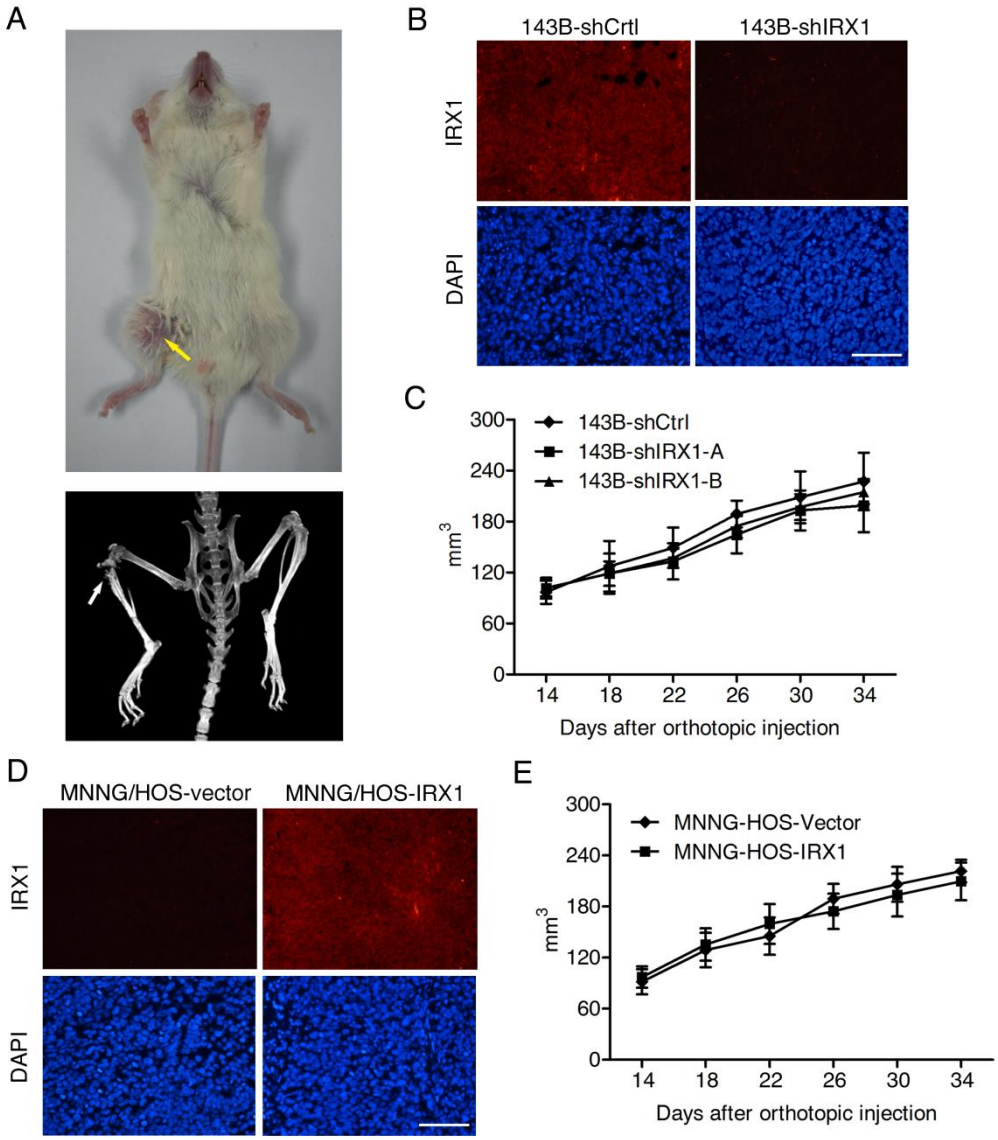

Supplemental Figure 4

IRX1 overexpression had no influence on tumor growth in an orthotopic model of osteosarcoma. The indicated 143B and MNNG/HOS cells were injected into the proximal tibia of NOD/SCID mice (n = 10), and the tumor volume was measured every 3 days. (A) A representative image of an orthotopic tumor (yellow arrow) in the right proximal tibia of NOD/SCID mice 5 weeks after injection. Bone destruction (white arrow) caused by the tumor growth was observed using a microPET-CT system. (B) Immunofluorescence analysis of IRX1 expression in tumors from mice bearing the indicated 143B cells. (C) IRX1 knockdown in 143B cells did not affect in vivo tumor growth. (D) Immunofluorescence analysis of IRX1 expression in tumors from mice bearing the indicated MNNG/HOS cells. (E) IRX1 overexpression in MNNG/HOS cells did not affect tumor growth. Scale bars: 100 μm.

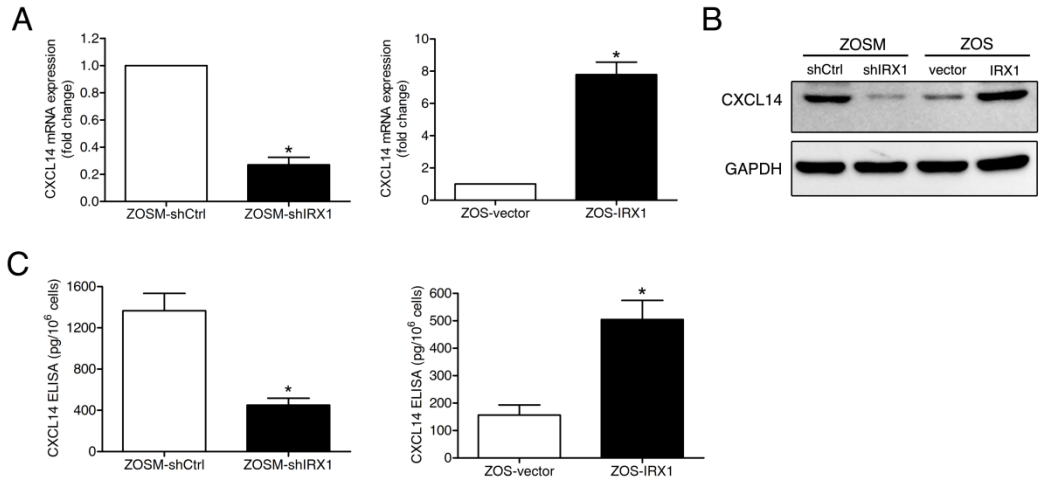

Supplemental Figure 5

CXCL14 expression was correlated with IRX1 expression in ZOS and ZOSM cells. CXCL14 mRNA (A), cellular protein (B), and secreted protein (C) levels in ZOS-IRX1 and ZOSM-shIRX1 cells were determined by real-time PCR, western blot and ELISA, respectively. Results shown in A and C are the mean ± SD (n=3). *P<0.05.

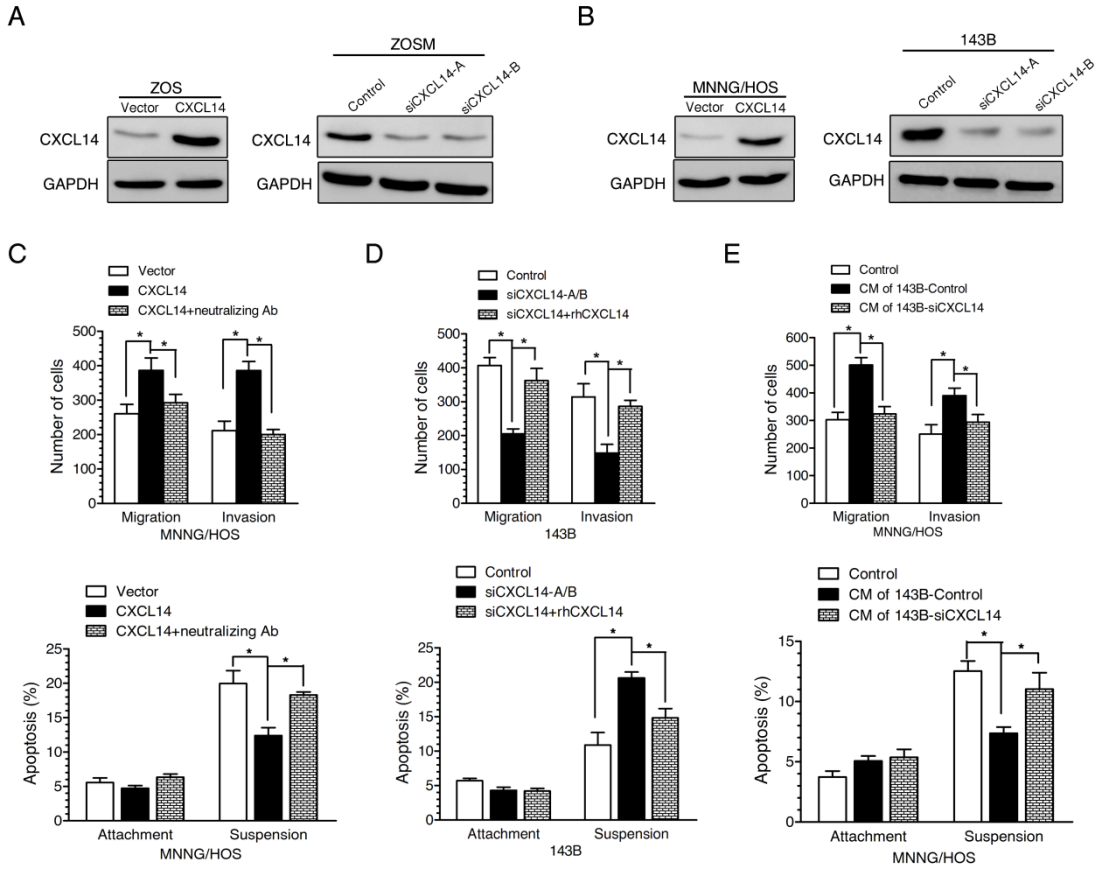

Supplemental Figure 6

CXCL14 promotes the metastatic ability of osteosarcoma cells in an autocrine manner. (A) The effect of CXCL14 overexpression and knockdown in ZOS and ZOSM cells was determined by western blot analysis. (B) The effect of CXCL14 overexpression and knockdown in MNNG/HOS and 143B cells was determined by western blot analysis. (C) Transwell and FACS assays were performed on control and CXCL14-overexpressing MNNG/HOS cells. A CXCL14-neutralizing antibody (20 μg/ml) was used to block the secreted CXCL14 in the culture medium of MNNG/HOS-CXCL14 cells. (D) Transwell and FACS assays were performed in control and CXCL14-knockdown 143B cells. Recombinant human CXCL14 (rhCXCL14, 200 ng/ml) was added to the culture medium of 143B-siCXCL14 cells. (E) Transwell and FACS assays were performed on MNNG/HOS cells cultured in conditioned medium (CM) from 143B-Control or 143B-siCXCL14 cells. The values shown are the mean ± SD of 3 separate determinations. **P*<0.05.

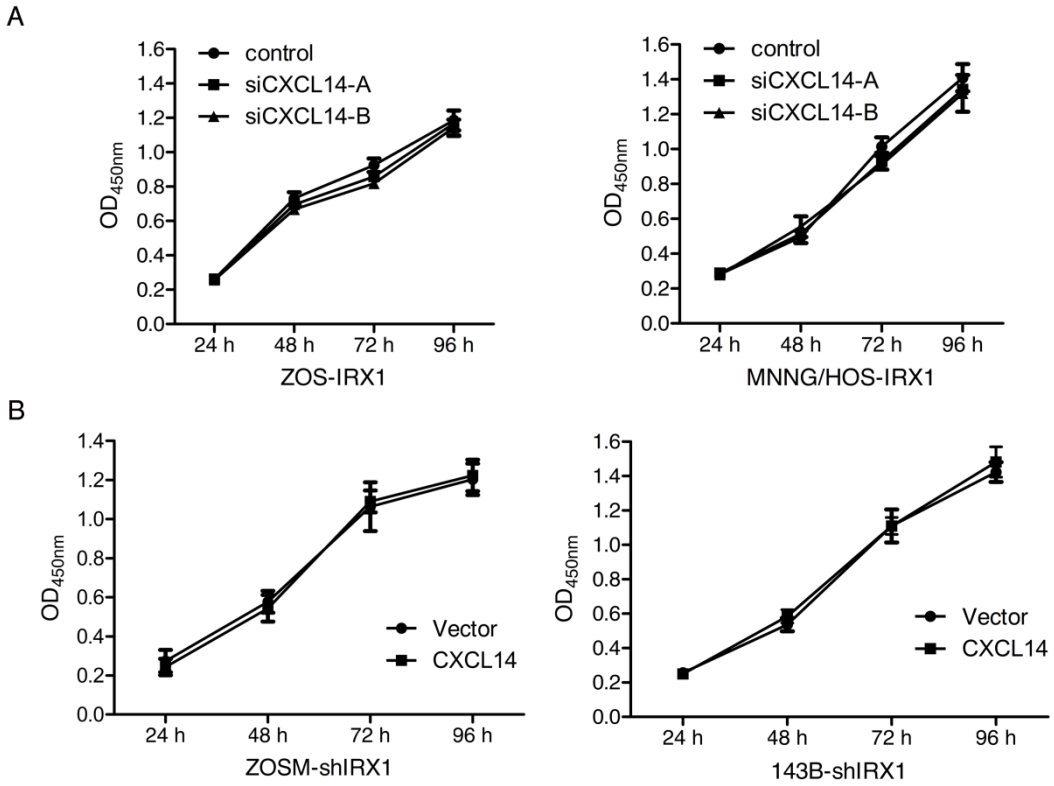

Supplemental Figure 7

CXCL14 did not affect the cell growth of IRX1-overexpressing or IRK1-knockdown osteosarcoma cells. (A) A Cell Counting Kit-8 assay was performed on control and CXCL14-knockdown ZOS-IRX1 and MNNG/HOS-IRX1 cells. (B) A Cell Counting Kit-8 assay was performed on control and CXCL14-overexpressing ZOSM-shIRX1 and 143B-shIRX1 cells. The values shown are the mean ± SD of 3 separate determinations.

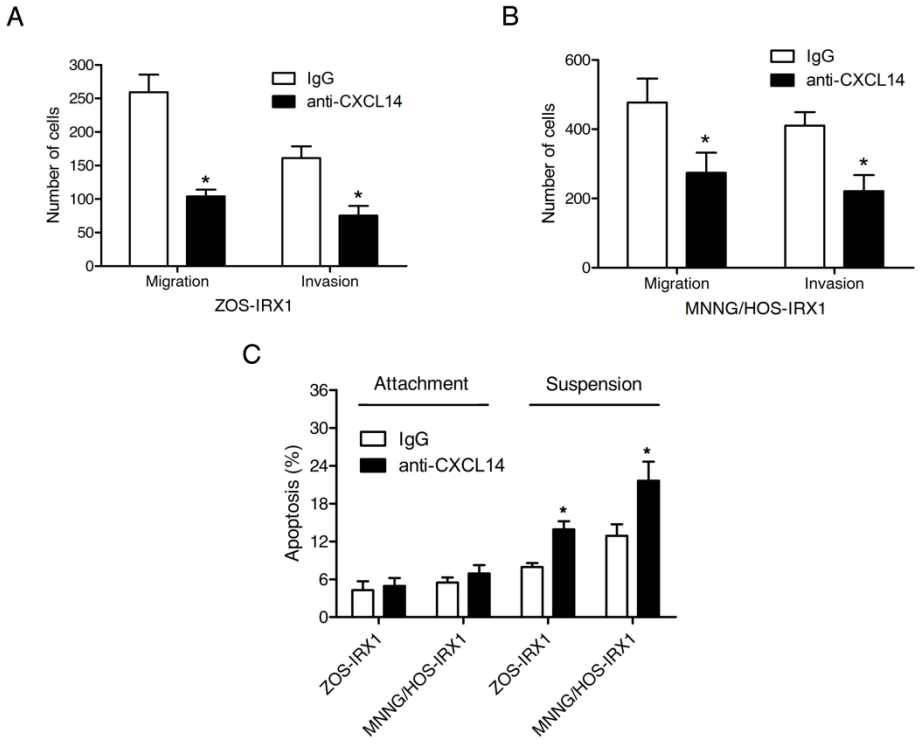

Supplemental Figure 8

CXCL14 blockade inhibited the migration, invasion and anoikis resistance in ZOS-IRX1 and MNNG/HOS-IRX1 cells. (A and B) The migration and invasion abilities of ZOS-IRX1 (A) and MNNG/HOS-IRX1 (B) cells after treatment with 20 μg/ml CXCL14-neutralizing antibody (R&D) or normal rat IgG (control, R&D) were tested in a Transwell assay. (C) FACS analysis showed that CXCL14 blockade by an anti-CXCL14 antibody (20 μg/ml) significantly increased the apoptotic rates of ZOS-IRX1 and MNNG/HOS-IRX1 cells in suspension culture conditions. The results shown in A-C represent the mean ± SD (n=3). *P<0.05.

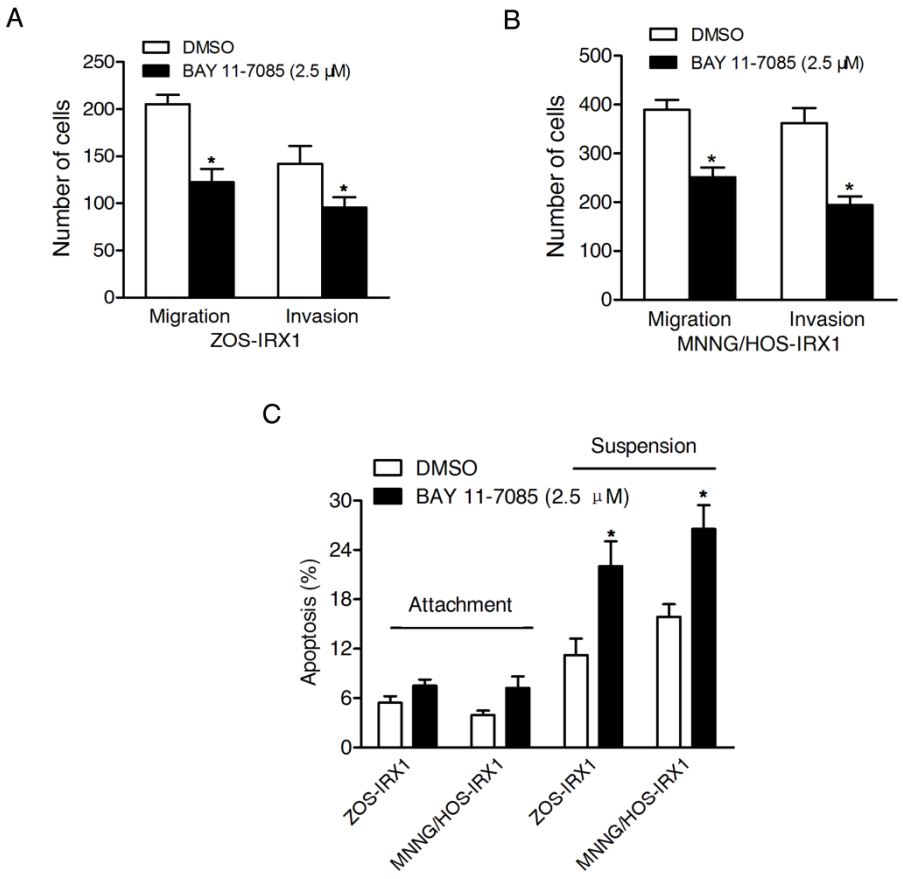

Supplemental Figure 9

BAY 11-7085 inhibited the migration, invasion and anoikis resistance of ZOS-IRX1 and MNNG/HOS-IRX1 cells. (A and B) Transwell assays were performed to determine the migration and invasion abilities of ZOS-IRX1 (A) and MNNG/HOS-IRX1 (B) cells after treatment with DMSO (control) or BAY 11-7085 (2.5 μM). (C) FACS analysis showed that BAY 11-7085 (2.5 μM) significantly increased the apoptotic rates of ZOS-IRX1 and MNNG/HOS-IRX1 cells in suspension culture. The results shown in A-C represent the mean ± SD (n=3). *P<0.05.

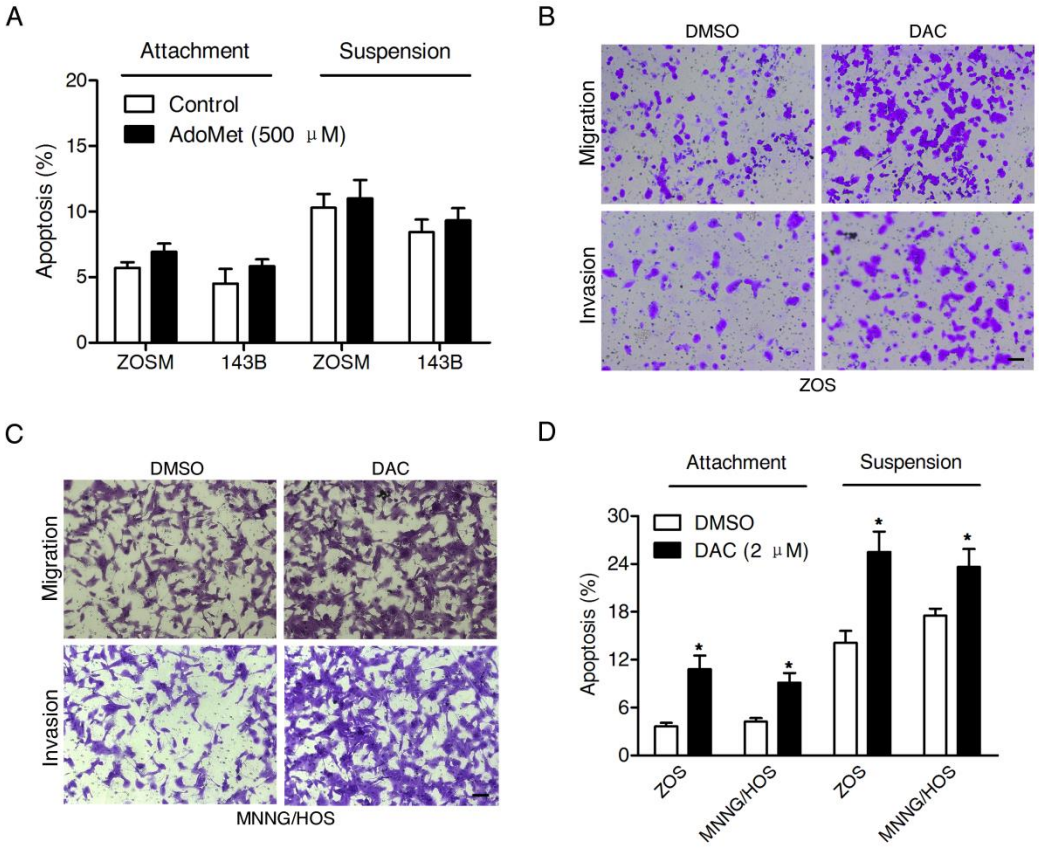

Supplemental Figure 10

The effect of AdoMet and DAC on osteosarcoma cells. (A) The apoptotic rates of ZOSM and 143B cells treated with AdoMet (500 μM) were determined by FACS under attached and suspension conditions. (B and C) Transwell assays were used to determine the migration and invasion abilities of ZOS (B) and MNNG/HOS (C) cells after treatment with DMSO (control) or DAC (2 μM) for 3 days. (D) The apoptotic rates of ZOS and MNNG/HOS cells treated with DAC (2 μM) for 3 days were determined by FACS. The results shown in A and D represent the mean ± SD (n=3). Scale bars: 100 μm.*P<0.05.

Supplemental Table 1 Microarray results (ZOSM vs. ZOS)

Gene	Title	Methylation[A]		Expression[B]	
		Location	Fold change	Accession No.	Fold change
Hypomethylated and upregulated					
SALL1	sal-like 1 (Drosophila)	promoter region	-4.32	NM_002968	11.83
IRX1	iroquois homeobox 1	promoter region	-3.59	AI870306	4.93
HOXB5	homeobox B5	promoter region	-2.97	NM_002147	2.49
CBR1	carbonyl reductase 1	promoter region	-2.47	BC002511	3.73
HOXB7	homeobox B7	promoter region	-2.43	AW102783	6.00
HOXA11	homeobox A11	promoter region	-2.37	H94842	4.52
COL16A1	collagen, type XVI, alpha 1	promoter region	-2.15	NM_001856	13.06
PRAME	preferentially expressed antigen in melanoma	promoter region	-1.95	NM_006115	10.34
NID2	nidogen 2 (osteonidogen)	promoter region	-1.90	NM_007361	3.84
CRABP2	cellular retinoic acid binding protein 2	promoter region	-1.84	NM_001878	5.24
ADM	adrenomedullin	promoter region	-1.69	NM_001124	3.14
EPCAM	epithelial cell adhesion molecule	promoter region	-1.68	NM_002354	2.95
CXCL6	chemokine (C-X-C motif) ligand 6	promoter region	-1.66	NM_002993	2.01
TSPAN11	tetraspanin 11	promoter region	-1.63	BE858239	2.29
STC2	stanniocalcin 2	promoter region	-1.55	AI435828	2.33
CAV1	caveolin 1, caveolae protein, 22kDa	promoter region	-1.49	NM_001753	17.49
SPHK1	sphingosine kinase 1	promoter region	-1.48	NM_021972	2.87
QPCT	glutaminyl-peptide cyclotransferase	promoter region	-1.44	NM_012413	5.81
Hypermethylated and downregulated					
FAM78A	family with sequence similarity 78, member A	promoter region	2.39	BF515132	-2.21
BEX5	brain expressed, X-linked 5	promoter region	1.88	AV726956	-5.16
SLC25A12	solute carrier family 25, member 12	promoter region	1.74	NM_003705	-3.50
PDGFD	platelet derived growth factor D	promoter region	1.64	AB033832	-2.21
PREX1	phosphatidylinositol-3,4,5-trisphosphate-dependent Rac exchange factor 1	promoter region	1.52	AL445192	-2.08
KCTD14	potassium channel tetramerization domain containing 14	promoter region	1.52	AI672101	-3.10
TSPAN31	tetraspanin 31	promoter region	1.49	NM_005981	-2.01
STAU2	staufen, RNA binding protein, homolog 2 (Drosophila)	promoter region	1.48	BC008370	-2.15

[A]MeDIP-chip data using a NimbleGen Human DNA Methylation 3x720K CpG Island Plus RefSeq Promoter Array. Data were stratified by a 1.4-fold change. [B]Gene expression microarray data using an Affymetrix Human Genome U133 Plus 2.0 Array. Candidate genes were considered significantly differentially expressed with a selection threshold of a 2-fold change.

Supplemental Table 2

Gene expression microarray results (143B-shIRX1 vs. 143B-shCtr)

Gene	Name	Accession no.	Locus	Fold change
Upregulated				
PASD1	PAS domain containing 1	BC040301	chrX	197.6
PADI2	peptidyl arginine deiminase, type II	BC009701	chr1	17.5
EREG	epiregulin	NM_001432	chr4	16.0
MIA	melanoma inhibitory activity	NM_006533	chr19	14.1
CCL20	chemokine (C-C motif) ligand 20	BC020698	chr2	13.4
MYEOV	myeloma overexpressed gene	NM_138768	chr11	11.6
MALL	mal, T-cell differentiation protein-like	BC003179	chr2	10.5
SLCO2A1	solute carrier organic anion transporter family, member 2A1	BC041140	chr3	8.6
KLRC1	killer cell lectin-like receptor subfamily C, member 1	NM_007328	chr12	8.2
MMP7	matrix metallopeptidase 7	NM_002423	chr11	8.2
CLDN1	claudin 1	NM_021101	chr3	7.2
KLRC2	killer cell lectin-like receptor subfamily C, member 2	NM_002260	chr12	6.9
KLRC3	killer cell lectin-like receptor subfamily C, member 3	AF461157	chr12	6.8
LIF	leukemia inhibitory factor	NM_002309	chr22	6.7
KLRC4	killer cell lectin-like receptor subfamily C, member 4	NM_013431	chr12	6.0
Downregulated				
LCE2A	late cornified envelope 2A	NM_178428	chr1	-12.2
GALC	galactosylceramidase	NM_000153	chr14	-11.4
IL1A	interleukin 1, alpha	NM_000575	chr2	-9.7
TSPYL5	TSPY-like 5	NM_033512	chr8	-8.9
EFS	embryonal Fyn-associated substrate	NM_005864	chr14	-5.9
C20orf39	chromosome 20 open reading frame 39	NM_024893	chr20	-5.6
MAFB	v-maf musculoaponeurotic fibrosarcoma oncogene homolog B	NM_005461	chr20	-5.6
CXCL14	chemokine (C-X-C motif) ligand 14	BC003513	chr5	-5.0
EDIL3	EGF-like repeats and discoidin I-like domains 3	BX648583	chr5	-4.9
CD3D	CD3d molecule, delta	NM_000732	chr11	-4.7
TXNIP	thioredoxin interacting protein	NM_006472	chr1	-4.4
HES5	hairy and enhancer of split 5 (Drosophila)	NM_001010926	chr1	-4.2
SPP1	secreted phosphoprotein 1	AK075463	chr4	-4.0
WDR66	WD repeat domain 66	NM_144668	chr12	-3.9
NPPB	natriuretic peptide precursor B	NM_002521	chr1	-3.9

Supplemental Table 3

Clinical characteristics of 113 osteosarcoma patients

	Total=113	Percentage (%)
Age (years)		
Average	18	
Range	5-49	
Gender		
Male	77	68.1
Female	36	31.9
Location		
Distal femur	64	56.6
Proximal tibia	29	25.7
Proximal humerus	10	8.9
Proximal femur	4	3.5
Other	6	5.3
Enneking		
IIB	85	75.2
III	28	24.8
Relapse		
Yes	7	6.2
No	106	93.8
Lung metastasis		
Yes	37	32.7
No	76	67.3
Death		
Yes	44	38.9
No	69	61.1

Supplemental Table 4

The association of IRX1 expression with patient clinicopathological characteristics in 113 osteosarcoma tissues

	Number	IRX1 expression level		*P* value*
		high	low	
Age				0.961
≤20	83	39	44	
21-40	28	14	14	
＞40	2	1	1	
Gender				0.258
Male	77	34	43	
Female	36	20	16	
Location				0.682
Distal femur	64	34	30	
Proximal tibia	29	12	17	
Proximal humerus	10	4	6	
Proximal femur	4	1	3	
Other	6	3	3	
Enneking				0.480
IIB	85	39	46	
III	28	15	13	
Relapse				0.708
Yes	7	4	3	
No	106	50	56	
Lung metastasis				**0.033**
Yes	37	23	14	
No	76	31	45	
Death				**0.007**
Yes	44	28	16	
No	69	26	43	

*Chi-square test

Supplemental Table 5

Multivariate analysis* of overall survival and metastasis in 113 osteosarcoma patients

	Variable	*RR*	95% *CI*	*P* value
Overall survival				
	Age	0.657	0.336-1.284	0.219
	Gender	0.590	0.293-1.189	0.140
	Location	0.983	0.741-1.303	0.904
	Enneking stage	1.328	0.687-2.570	0.399
	IRX1	2.252	1.204-4.212	0.011
Lung metastasis				
	Age	0.696	0.344-1.409	0.314
	Gender	0.966	0.481-1.940	0.922
	Location	0.957	0.700-1.307	0.781
	Enneking stage	4.407	2.256-8.606	0.000
	IRX1	2.482	1.252-4.918	0.009

*Cox proportional hazards regression

Supplemental Table 6

Primers used in this study

Gene	Sequence (5' to 3')
Real-time PCR	
IRX1-F	GGAATGTGGGAGGAATTAAGAC
IRX1-R	GCATTTACCGAACCCGATA
CXCL14-F	CTGCGAGGAGAAGATGGTTA
CXCL14-R	CTTTGCACAAGTCTCCCAAC
GAPDH-F	AGAAAAACCTGCCAAATATGATGAC
GAPDH-R	TGGGTGTCGCTGTTGAAGTC
SALL1-F	TCTGCCCCAGCTGATGTT
SALL1-R	TAGTAGGGCGACTCGGTTG
HOXB5-F	TGAGGAAGCTTCACATCAGC
HOXB5-R	AACTCCTTTTCCAGCTCCAG
CBR1-F	TCTTTGGTACCCGAGATGTG
CBR1-R	GGCTGCAGCTTTTAAGGG
HOXB7-F	ACCGACACTAAAACGTCCCTGCC
HOXB7-R	GAAGGCTCCGGTAGCGAAAACC
HOXA11-F	AAGAGGCAGCTGCAGTGGAGAATC
HOXA11-R	GGCAAATACATGTTAGAGGAGCAGGG
COL16A1-F	ACTTTGGATGGGCAGCTC
COL16A1-R	CAAACCGTTGTTTCCAGGC
PRAME-F	AGGCTTCAGGGTACAGCTC
PRAME-R	TCCTCAGAGAGTTCACCACAC
NID2-F	GCAGATCACTTCTACCACACAG
NID2-R	CGTAGAGGTGAGATCGTTGTTC
CRABP2-F	GATTCAAGTGCTGGCTTTGCGTC
CRABP2-R	TTCTCTGGATCTAGCCCGCGTG
ADM-F	GGAAAGAAAGGGAAGGCAACCG
ADM-F	CAAACACACTCACATTCCACGCG
EPCAM-F	GCCGCAGCTCAGGAAGAATGTG
EPCAM-R	CATTTGGCAGCCAGCTTTGAGC
CXCL6-F	ACCCCTTCTTTCCACACTGCCC
CXCL6-R	ACTTTGGTTTCCTCGTGCCTTCTG
TSPAN11-F	TAAGACTGAGCAGGACGACTGGCTG
TSPAN11-R	GAGGTAGCCACTCTTCTCCACCAGG
STC2-F	GTGAGATTCGGGGCTTACAT
STC2-R	GCCTTACATTTCAAGGCGTC
CAV1-F	AGTTTTCATCCAGCCACGG
CAV1-R	TGGGCTTGTAGATGTTGCC
SPHK1-F	ACCGATAAGGAGCTGAAGGCAGG
SPHK1-R	CGCTGGATCCATAACCTCGACC
QPCT-F	GCTCCAAACCCAACGTTTC
QPCT-R	AGTGATCCTTGAGCAAACCC

FAM78A-F	TGAGGCACAGAAGGGCTGGATG
FAM78A-R	CCCTGGGCTCTCTCTTCTTCTCCTC
BEX5-F	GGGCAATGTCTGATGGAGTC
BEX5-R	GAGGCAGTCTTTCTCTCTTAGC
SLC25A12-F	GAGTGGAAATGGAGAGGTGAC
SLC25A12-R	ATGCTTCTTCCGGTTATGCC
PDGFD-F	TCTTCTTTCCACGTTGCCTC
PDGFD-R	GGCCAGGCTCAAACTGTAAT
PREX1-F	CTTCGCAACGACTTCAAGC
PREX1-R	GTCAAAGCCATAGTCCTCCTC
KCTD14-F	GGCCCAAGTGATCTGCATGTGG
KCTD14-R	CCGACGTTCAGCTCCACAACAGTAG
TSPAN31-F	CGCTCTCAACGTGGTCTAC
TSPAN31-R	AAGACTCCCACAGCAATGAC
STAU2-F	CCCGTTTCAATAGAGTCCAACC
STAU2-R	GATTCCCATGTCTGCTCACC

Methylation

BSP-F	TGTTAAAGATGTTTTTTGGAGGTTT
BSP-R	AATATATCCCCTTTTTAACAAAAACAAC
MSP (M)-F	GTTAAAGATGTTTTTTGGAGGTTTC
MSP (M)-R	ATCTAACACCGAATTTACAATTTCG
MSP (U)-F	TTAAAGATGTTTTTTGGAGGTTTTG
MSP (U)-R	CTATCTAACACCAAATTTACAATTTCAC

MassARRAY

IRX1-F	TTGTTAAAGATGTTTTTTGGAGGTT
IRX1-R	AAATATATCCCCTTTTTAACAAAAACAA

shRNA

shIRX1-A-F	TTCTCAGCCTCTTCTCGCAGATCTCGAGATCTGCGAGAAGAGGCTGAGATTTTTC
shIRX1-A-R	TCGAGAAAAATCTCAGCCTCTTCTCGCAGATCTCGAGATCTGCGAGAAGAGGCTGAGAA
shIRX1-B-F	TCATTGACAAGATCGACGAGCACTCGAGTGCTCGTCGATCTTGTCAATGTTTTTC
shIRX1-B-R	TCGAGAAAAACATTGACAAGATCGACGAGCACTCGAGTGCTCGTCGATCTTGTCAATGA
shCXCL14-A-F	TGCTTCATCAAGTGGTACAACTCGAGTTGTACCACTTGATGAAGCTTTTTC
shCXCL14-A-R	TCGAGAAAAAGCTTCATCAAGTGGTACAACTCGAGTTGTACCACTTGATGAAGCA
shCXCL14-B-F	TGACGTGAAGAAGCTGGAAACTCGAGTTTCCAGCTTCTTCACGTCTTTTTC
shCXCL14-B-R	TCGAGAAAAAGACGTGAAGAAGCTGGAAACTCGAGTTTCCAGCTTCTTCACGTCA

siRNA

siCXCL14-A-F	GCGAGGAGAAGAUGGUUAUTT
siCXCL14-A-R	AUAACCAUCUUCUCCUCGCTT
siCXCL14-B-F	GGGUCCAAAUGCAAGUGCUTT
siCXCL14-B-R	AGCACUUGCAUUUGGACCCTT

ChIP

site A-F	AGACAGGCCTCAAAGCAA
site A-R	ATTGGCACCATCGTTTTATGTC
site B-F	TATTTCTGAGGGCTGATCCAATG
site B-R	GTGCTGACCATTGCGGTT
HEBP1-F	AGGGATGGTAGGAAAGAGTGG
HEBP1-R	TGTCTTGGTAGCTGTCCCTC
BDKRB2-F	TGGGGCTTCCCAGGCCACTT
BDKRB2-R	GCCACCTTCGCTCTCCGCTC

Supplemental Methods

Cell lines

The MNNG/HOS and 143B cell lines were purchased from the American Type Culture Collection (ATCC) and were cultured according to the instructions provided by the ATCC. The syngeneic human osteosarcoma cell lines ZOS and ZOSM, which were derived from primary tumor and skip metastases in the same patient, were established at our institution (1). The primary cell cultures were grown in DMEM (Gibco) supplemented with 10% FBS (Gibco) at 37 ℃ with 5% CO_2.

Reagents

5-Aza-2'-deoxycytidine (Sigma-Aldrich), S-adenosyl-L-methionine (Sigma-Aldrich), recombinant human CXCL14 (R&D, #866-CX-025), human CXCL14 affinity-purified polyclonal antibody (R&D, #AF866), normal rat IgG control (R&D, #6-001-A), and BAY 11-7085 (Selleck, 10 μM stock in DMSO, #S2913).

Patients and tissue samples

The medical charts of the osteosarcoma patients included in this study were reviewed. All patients received standard neoadjuvant chemotherapy that was followed by surgical resection and postoperative chemotherapy. The primary osteosarcoma tissues were collected when surgical resection of the primary tumor was performed, and metastatic tissues were obtained when pulmonary metastasectomy was performed after the primary tumor was under control. The formalin-fixed, paraffin-embedded surgical specimens were stored in the tissue bank of the Department of Pathology. Fresh tumor specimens were snap-frozen in liquid nitrogen immediately after surgical resection and stored at –80 ℃ in our department. Osteosarcoma was confirmed histopathologically, and only tumor samples that were composed of >80% tumor cells were used for the real-time PCR study. Serum samples were obtained on the date of diagnosis before any initial treatment.

Methylated DNA immunoprecipitation (MeDIP) assay

The MeDIP assay was performed as previously described with some modifications (2). Briefly, genomic DNA extracted from ZOS and ZOSM cell lines was digested into 200–1000-bp fragments using MseI. The digested fragments were then denatured and incubated with a monoclonal antibody against 5-methylcytidine. Subsequently, MeDIP samples were amplified and labeled with Cy5 (IP DNA) or Cy3 (Input DNA) dyes. A hybridization system (NimbleGen) was then used to co-hybridize the labeled samples to the Human DNA Methylation 3×720K CpG Island Plus RefSeq Promoter Array, which contains 50-75 monomer oligonucleotide probes covering the region from −2440 bp to +610 bp relative to the potential transcription start sites for 22532 annotated human genes. The arrays were then washed and scanned with the MS200 scanner (NimbleGen). Data were collected and normalized for comparisons of fold enrichment. The methylation level was found to be significantly different between ZOS and ZOSM cells; a 1.4-fold change was considered to be the selection threshold. The data set has been uploaded to the Gene Expression Omnibus under accession number GSE55961.

Gene expression profiling

Microarray analysis was performed using the Affymetrix Human Genome U133 Plus 2.0 Array (ZOS vs. ZOSM) and NimbleGen Human Gene Expression 12×135K Array (143B-shCtrl vs. 143B-shIRX1), as described previously (3, 4). The selection threshold used to determine significantly differentially expressed genes was a false discovery rate (FDR) <5% and a fold change ＞2.0 in the SAM output result. The microarray data sets have been submitted to the Gene Expression Omnibus with the accession numbers GSE55957 and GSE55958.

Real-time RT-PCR

Total RNA from osteosarcoma cell lines and tissue samples was purified using the RNeasy Mini Kit (Qiagen), and first strand cDNA was synthesized using the First Strand cDNA Synthesis Kit (Fermentas) according to the manufacturer's instructions. Real-time RT-PCR was carried out using SYBR® qPCR Mix (Toyobo) according to the manufacturer's protocol with a Bio-Rad iQ5 Real-Time PCR Detection System. The sequences of the primers used for PCR are shown in Supplemental Table 6. The experiments were performed in triplicate.

Western blot analysis

Western blot analysis was performed using standard procedures. Briefly, 60 μg of protein extracted from cultured cells was separated by 12-15% SDS-PAGE and transferred to PVDF membranes. The membranes were blocked in 5% nonfat dry milk and then incubated with the antibodies as follow: IRX1 (1:500, Bioworld, #BS2291), CXCL14 (1:1000, Abcam, #ab46010), NF-κB p65 (1:5000, Abcam, #ab32536), IκBα (1:5000, Abcam, #ab32518), MMP9 (1:500, Bioworld, #BS6893), c-FLIP (1:1000, Abcam, #ab167409), H2AX (1:1000, Abcam, #ab124781), GAPDH (1:5000, Bioworld, #AP0066). Subsequently, the membranes were incubated with horseradish peroxidase-conjugated secondary antibody for 1 hour at room temperature. The protein bands were visualized with the enhanced chemiluminescence detection system using a GE ImageQuant LAS4000 mini.

5-Aza-2'-deoxycytidine (DAC) and S-adenosyl-L-methionine (AdoMet) treatment

Cultured cells were treated with varying concentrations of DAC (0.5, 1, 2, 5, or 10 μM) or AdoMet (50, 100, 200, or 500 μM) as previously described (5, 6). Briefly, cells were seeded at a density of 3×10^5 in 100-mm dishes with 10 ml of growth medium, cultured overnight, and treated with different concentrations of freshly prepared DAC (Sigma-Aldrich) for 3 days without changing the medium or treated with AdoMet (Sigma-Aldrich) for 6 days with the medium changes every other day. The cells were harvested by trypsinization for RNA, DNA and protein extraction.

Bisulfite sequencing PCR (BSP) and methylation-specific PCR (MSP)

Bisulfite sequencing PCR and methylation-specific PCR were performed to analyze the methylation status of the IRX1 promoter as previously described (7, 8). Briefly, genomic DNA was isolated from cultured cells using a DNeasy Blood & Tissue Kit (Qiagen), and the cell-free DNA from serum samples was extracted using a QIAamp DNA Blood Mini Kit (Qiagen). The isolated DNA was then bisulfite converted and purified using EpiTect Bisulfite Kits (Qiagen) according to the manufacturer's instructions. For BSP, PCR primers (Supplemental Table 6) were designed to amplify the modified IRX1 promoter (-521 to -679). The amplified PCR products

were purified with a QIAquick Gel Extraction Kit (Qiagen) and cloned into the pMD19-T vector (Takara) followed by sequencing analysis.

Methylation-specific PCR was performed with the EpiTect MSP kit (Qiagen) according to the manufacturer's instructions. The PCR primers are shown in Supplemental Table 6. The PCR products were separated on a 2% agarose gel with DuRed and directly visualized under UV illumination. Completely methylated and unmethylated DNA fragments (from the EpiTect PCR control DNA set (Qiagen)) were used as positive and negative controls, respectively.

MassARRAY

Quantitative analysis of IRX1 promoter methylation (-520 to -680) was performed using the MassARRAY Compact System (Sequenom) as described previously (9). Briefly, genomic DNA was prepared from osteosarcoma tissues using the DNeasy Blood & Tissue Kit (Qiagen). The DNA was then bisulfite converted and amplified by PCR. The primers for PCR amplification are listed in Supplemental Table 6. After treatment with shrimp alkaline phosphatase, the PCR products were transcribed in vitro, cleaved with RNase A and then subjected to MALDI-TOF-MS (Sequenom). The results were analyzed using EpiTyper software v1.0 (Sequenom), and the methylation level was calculated as the average values of the CpG units (units 1, 2, 4 and 6).

In vitro *methylation*

A 159-bp fragment of the IRX1 promoter region (-521 to -679) was obtained via whole gene synthesis (BGI, Beijing, China) and subsequently methylated in vitro with *Sss*I, *Hpa*II and *Hha*I methylases (New England Biolabs) according to the manufacturer's instructions. *Sss*I methylates all cytosine residues within the 5'-CpG-3' sequence, *Hpa*II methylates cytosine residues within 5'-CCGG-3', and *Hha*I methylates cytosine residues within 5'-GCGC-3'. Complete methylation was confirmed by digestion with *Hha*I, *Hpa*II, and *Mcr*BC (New England Biolabs). Methylated or mock-methylated fragments were ligated into the pGL3-basic vector (Promega) for luciferase reporter assays.

Lentiviral transduction studies

Lentivirus packing expression vectors (pLenti.neo-shIRX1/shCXCL14-eGFP and pLV.EX3d.P/neo-EF1A>IRX1/CXCL14>IRES/eGFP) were obtained from Cyagen Biosciences (Guangzhou, China). To generate the stable knockdown and overexpression lines, osteosarcoma cells were transduced with the indicated lentiviruses (MOI=10~20). The transduction efficiency was assayed by imaging with an inverted fluorescence microscope (Leica), and the stable clones were selected with 1 mg/ml G418 (Sigma Aldrich). Real-time RT-PCR and immunoblotting for IRX1 and CXCL14 were performed to determine the knockdown and overexpression efficiency. The shRNA sequences are shown in Supplemental Table 6.

Transient transfection

Small interfering RNA (siRNA) targeted against CXCL14 was synthesized by GenePharma (Suzhou, China). The target sequences are listed in Supplemental Table 6. Plasmids encoding human CXCL14 were obtained from Cyagen Biosciences (Guangzhou, China). The cells were transfected with targeting siRNA or expression plasmids using Lipofectamine 2000 (Invitrogen) according to the manufacturer's instructions.

Cell Counting Kit-8 assay (CCK8)

Cell suspensions (100 μl) were plated at a density of 2000 cells per well in 96-well plates. After incubation for the indicated time periods (24 h, 48 h, 72 h and 96 h), 10 μl of CCK-8 solution (Beyotime) was added to each well of the plate. The plate was incubated for an additional 4 h, and the absorbance was measured at 450 nm using a SUNRISE Absorbance Reader (TECAN). The experiments were performed in triplicate.

Wound healing assays

Cells were plated in 6-well plates (3×10^5 cells/well). When the cells reached 90% confluence, a scratch was made using a sterile 200-μl pipette tip, and the detached cells were removed by washing with culture medium. Phase contrast images were obtained in the same field at 0 h, 24 h, 36 h and 48 h using an inverted microscope (Leica). The experiments were performed in triplicate.

Boyden chamber migration and invasion assays

Cell migration and invasion assays were performed using 24-well transwells (8.0-μm pore size) with or without Matrigel coating (Becton Dickinson). In total, 2.0×10^4 cultured cells in 0.2 ml of serum-free DMEM were seeded in the upper chamber, and 0.6 ml of DMEM containing 10% fetal bovine serum was added to the lower chamber. After 12 or 24 h of incubation, the cells remaining in the upper chamber were removed with cotton swabs, and the filters were fixed with 4% paraformaldehyde for 15 min followed by crystal violet staining and microscopic examination. The migrating or invading cells in five random optical fields (× 100 magnification) from triplicate filters were counted and averaged.

Anoikis assay

To prevent cell adhesion, cells were seeded at a density of 2×10^5 cells per well in 6-well ultra-low-attachment culture plates (Corning). After incubation for 48 h, the cells were harvested and stained with the Annexin V Apoptosis Detection Kit APC (eBioscience). The apoptosis rate was determined by fluorescence-activated cell sorting (FACS) analysis. The experiments were performed in triplicate.

Luciferase reporter assays and chromatin immunoprecipitation (ChIP)

For luciferase reporter assays, cells were seeded at a density of 4×10^4 cells/well in 24-well plates and co-transfected with pGL3-basic, the methylated plasmid pGL3-IRX1 (-521 to -679) or pGL3-CXCL14 (–2000 to +515), a NF-κB p65 luciferase reporter (Beyotime) or the pRL-TK plasmid (Promega) using Lipofectamine 2000 (Invitrogen). After 48 hours, the cells were harvested in Passive Lysis Buffer (Promega). Luciferase activity was measured using the Dual Luciferase Reporter Assay System (Promega) with a GloMax Luminometer (Promega). The results were quantified as the ratio of firefly luciferase/Renilla luciferase activity.

ChIP was performed using the Pierce™ Agarose ChIP Kit (Thermo) as described by the manufacturer. Briefly, 143B cells in a 10-cm dish were cross-linked with 1% formaldehyde, and fixation was terminated with a glycine solution. The cells were harvested and incubated in lysis buffer with micrococcal nuclease for digestion. The samples were immunoprecipitated overnight at 4°C with 5 μg anti-IRX1 antibody (Abnova, #H00079192-A01) and 2 μg of normal rabbit IgG (R&D, #6-001-A). Protein A/G Plus Agarose was added and incubated at 4℃ for 1 hour. The

immune complexes were then washed and eluted. DNA was recovered and purified using the DNA Clean-Up Column supplied in the ChIP Kit. The immunoprecipitated DNA was analyzed by real-time RT-PCR. BDKRB2, which has been demonstrated to be a direct target of IRX1 (10), was used as a positive control; HEBP1, whose promoter has no potential IRX1 binding sites, was used as a negative control. The primers are shown in Supplemental Table 6.

Enzyme-linked immunosorbent assay (ELISA)

The levels of CXCL14 in the cell culture supernatants were determined using the Human CXCL14/BRAK DuoSet (R&D, #DY866) according to the manufacturer's recommendations. Briefly, 100 µl aliquots of the samples or standards (recombinant human CXCL14, R&D) were incubated for 2 hours at room temperature in 96-well plates (Corning) precoated with a capture antibody. After washing three times with phosphate-buffered saline containing 0.05% Tween-20, biotinylated mouse anti-human CXCL14 (R&D) was added to each well and incubated for 2 hours at room temperature. After three washes, streptavidin conjugated to horseradish peroxidase was added, followed by incubation with the substrate solution for 20 minutes. The optical density of each well was determined immediately after adding the stop solution using a microplate reader (TECAN) at 450 nm with a wavelength correction of 540 nm. The concentration of CXCL14 in the samples was estimated by referring to the standard curve using Sigmaplot 11.0 software (Systat Software Inc., San Jose, CA).

Immunohistochemistry and immunofluorescence

The paraffin-embedded osteosarcoma tissues were sectioned at 5 µm, and the sections were then de-waxed in xylene and rehydrated in graded alcohols. Endogenous peroxidase activity was quenched via incubation with 3% hydrogen peroxide for 5 minutes. Antigen retrieval was performed by incubating the slides with pepsin (Dako) at 37℃ for 10 min. The sections were incubated with antibodies against IRX1 (1:200, Bioworld, #BS2291), CXCL14 (1:200, Abcam, #ab46010) or MMP9 (1:100, Bioworld) at 4℃ overnight. For immunohistochemistry, primary antibodies were detected with the Dako EnVision Kit (Dako) according to the manufacturer's protocol. The staining intensity was evaluated and scored by 2 independent pathologists. The extent of staining was scored as previously described (11): 0: 0% of cells stained, 1: <5% of cells stained, 2: 5–50% of cells stained, or 3: >50% of cells stained. Staining intensity was scored as 0: negative, 1: weak, 2: intermediate or 3: strong. The final staining score was defined as the sum of the extent and intensity scores and categorized as low (scores 0 and 2) or high (3–6) expression.

For immunofluorescence, osteosarcoma cells and tissue sections were incubated with IRX1 (1:100, Santa Cruz, #sc-22578) or CXCL14 (1:100, Abcam, #ab46010) antibodies. Donkey anti-goat IgG (Alexa Fluor® 555, Abcam, #ab150130) and goat anti-rabbit IgG (Alexa Fluor® 488, Abcam, #ab150077) secondary antibodies were used, and the nuclei were counterstained with DAPI (Sigma-Aldrich). Immunofluorescence was detected with a BX51WI Fixed Stage Upright Microscope (Olympus).

References

1. Zou CY, Wang J, Shen JN, Huang G, Jin S, Yin JQ, Guo QC, Li HM, Luo L, Zhang M, et al. Establishment and characteristics of two syngeneic human osteosarcoma cell lines from primary tumor and skip metastases. *Acta Pharmacol Sin.* 2008;29(3):325-32.

2. Weng YI, Huang TH, and Yan PS. Methylated DNA immunoprecipitation and microarray-based analysis: detection of DNA methylation in breast cancer cell lines. *Methods Mol Biol.* 2009;590:165-76.
3. Bauer M, Su G, Casper C, He R, Rehrauer W, and Friedl A. Heterogeneity of gene expression in stromal fibroblasts of human breast carcinomas and normal breast. *Oncogene.* 2010;29(12):1732-40.
4. Xu PB, Lou JS, Ren Y, Miao CH, and Deng XM. Gene expression profiling reveals the defining features of monocytes from septic patients with compensatory anti-inflammatory response syndrome. *J Infect.* 2012;65(5):380-91.
5. Al-Romaih K, Somers GR, Bayani J, Hughes S, Prasad M, Cutz J-C, Xue H, Zielenska M, Wang Y, and Squire JA. Modulation by decitabine of gene expression and growth of osteosarcoma U2OS cells in vitro and in xenografts: Identification of apoptotic genes as targets for demethylation. *Cancer Cell Int.* 2007;7(1):14.
6. Pakneshan P, Szyf M, Farias-Eisner R, and Rabbani SA. Reversal of the hypomethylation status of urokinase (uPA) promoter blocks breast cancer growth and metastasis. *J Biol Chem.* 2004;279(30):31735-44.
7. Wu H, Chen Y, Liang J, Shi B, Wu G, Zhang Y, Wang D, Li R, Yi X, Zhang H, et al. Hypomethylation-linked activation of PAX2 mediates tamoxifen-stimulated endometrial carcinogenesis. *Nature.* 2005;438(7070):981-7.
8. Nakayama H, Hibi K, Takase T, Yamazaki T, Kasai Y, Ito K, Akiyama S, and Nakao A. Molecular detection of p16 promoter methylation in the serum of recurrent colorectal cancer patients. *Int J Cancer.* 2003;105(4):491-3.
9. Ehrich M, Nelson MR, Stanssens P, Zabeau M, Liloglou T, Xinarianos G, Cantor CR, Field JK, and van den Boom D. Quantitative high-throughput analysis of DNA methylation patterns by base-specific cleavage and mass spectrometry. *Proc Natl Acad Sci U S A.* 2005;102(44):15785-90.
10. Jiang J, Liu W, Guo X, Zhang R, Zhi Q, Ji J, Zhang J, Chen X, Li J, Zhang J, et al. IRX1 influences peritoneal spreading and metastasis via inhibiting BDKRB2-dependent neovascularization on gastric cancer. *Oncogene.* 2011;30(44):4498-508.
11. Zhao Z, Wu MS, Zou C, Tang Q, Lu J, Liu D, Wu Y, Yin J, Xie X, Shen J, et al. Downregulation of MCT1 inhibits tumor growth, metastasis and enhances chemotherapeutic efficacy in osteosarcoma through regulation of the NF-kappaB pathway. *Cancer Lett.* 2014;342(1):150-8.